

---

Proceedings of the XXVIII International School of Semiconducting Compounds, Jaszowiec 1999

## DEFECTS AND DEFECT REACTIONS IN SEMICONDUCTOR NITRIDES

C.G. VAN DE WALLE<sup>a</sup>, J. NEUGEBAUER<sup>b</sup>, C. STAMPFL<sup>b\*</sup>, M.D. MCCLUSKEY<sup>c</sup>  
AND N.M. JOHNSON<sup>a</sup>

<sup>a</sup>Xerox Palo Alto Research Center, 3333 Coyote Hill Road, Palo Alto, CA 94304, USA

<sup>b</sup>Fritz-Haber-Institut der Max-Planck-Gesellschaft  
Faradayweg 4-6, 14 195 Berlin-Dahlem, Germany

<sup>c</sup>Department of Physics, Washington State University  
P.O. Box 642814, Pullman, WA 99164-2814, USA

We report a comprehensive investigation of native point defects and impurities in GaN, AlN, and AlGaIn alloys, with the goal of understanding doping limitations in nitride semiconductors. Unintentional incorporation of impurities (mainly oxygen) explains the tendency of nitride semiconductors to exhibit *n*-type conductivity. Silicon is the *n*-type dopant of choice; it remains shallow in AlGaIn up to high Al content, while oxygen undergoes a DX transition. Experimental evidence for DX centers will be discussed. In *p*-type material, Mg doping is hindered by an increase in ionization energy with increasing Al content in AlGaIn, and by nitrogen vacancies acting as compensating centers. Complex formation between magnesium and oxygen and between magnesium and nitrogen vacancies will be discussed.

PACS numbers: 61.72.Bb, 61.72.Ji, 61.82.Fk, 71.55.Eq

### 1. Introduction

Nitride semiconductors have recently been demonstrated to have great potential for technological applications, ranging from blue light emitters to high-temperature and high-frequency devices. Native point defects have always been assumed to play an important role in the properties of nitrides. Nitrogen vacancies were long considered to be the source of *n*-type conductivity. Systematic investigations have now revealed that this is not the case. Based on first-principles calculations, we argued that the nitrogen vacancy concentration is too low to have any serious impact on doping of *n*-type material [1]. The methodology of these calculations is described in Sec. 2. We proposed that the observed unintentional *n*-type conductivity is due to incorporation of impurities (mainly silicon and oxygen). In Sec. 3, we will describe the experimental evidence that is now available

---

\*Present address: Department of Physics and Astronomy, Northwestern University, Evanston, Illinois 60208-3112, USA.

concerning the incorporation of these impurities. In particular, we will discuss hydrostatic pressure experiments that have shown a conversion from a shallow to a deep donor level upon application of hydrostatic pressure. This behavior was initially interpreted as evidence for the presence of nitrogen vacancies; we show, however, that the observations are consistent with oxygen undergoing a transition to a DX center. Analogous behavior is observed for donors in  $\text{Al}_x\text{Ga}_{1-x}\text{N}$  alloys, in which a similar shallow-to-deep transition for oxygen is observed when the Al content exceeds 30%. These findings are of high importance for devices in which AlGaIn alloys with high Al content are used as *n*-type layers. We predict that silicon donors will *not* undergo the DX transition, a prediction that so far has been experimentally verified in AlGaIn layers with Al content up to 60% [2].

In Sec. 4 we focus on the behavior of *p*-type material. The nitrogen vacancies, which played no significant role in *n*-type material, now may occur in larger concentrations, and could act as compensating centers. The presence of hydrogen, abundantly available during metal-organic chemical vapor deposition (MOCVD) and hydride vapor phase epitaxy (HVPE) growth, tends to suppress the formation of vacancies, but some degree of compensation is unavoidable. We have also investigated the behavior of the Mg acceptor and of the compensating defects in AlGaIn. We discuss how nitrogen vacancies may play a role in the blue luminescence that is commonly observed in Mg-doped GaN. Complexes can also be formed consisting of a nitrogen vacancy with one hydrogen (the maximum number that can be accommodated in the vacancy). We will discuss how these complexes behave during the annealing process used to activate *p*-type GaN, and why they may be responsible for the observed shift in luminescence lines. We will also describe the role of nitrogen vacancies as metastable centers responsible for persistent photoconductivity, and for the commonly observed blue emission in *p*-type GaN. Finally, we discuss complex formation between Mg acceptors and nitrogen vacancies, and between Mg and oxygen.

A general finding from our first-principles calculations for GaN [3], AlN [4], and InN [5] is that self-interstitials and antisites are always high in energy (with the exception of the Al interstitial in *cubic* AlN, which is a triple donor and could act as a compensating center in *p*-type material). It is therefore safe to concentrate on the properties of vacancies as the relevant native point defects in nitride semiconductors.

## 2. Methodology

The equilibrium concentration of a defect (or impurity) in a semiconductor is given by

$$c = N_{\text{sites}} \exp(-E^{\text{f}}/kT), \quad (1)$$

where  $E^{\text{f}}$  is the formation energy, and  $N_{\text{sites}}$  is the number of sites the defect or impurity can be incorporated on. For instance, for a nitrogen vacancy in GaN  $N_{\text{sites}}$  is equal to the number of nitrogen sites in the crystal, about  $4.4 \times 10^{22} \text{ cm}^{-3}$ .  $k$  is the Boltzmann constant, and  $T$  the temperature. Equation (1) shows that defects with a *high* formation energy will occur in *low* concentrations.

The formation energy of a defect in charge state  $q$  is expressed as

$$E^f(q) = E_{\text{defect}}^{\text{tot}}(q) - \sum_X n_X \mu_X + qE_F, \quad (2)$$

where  $E_{\text{defect}}^{\text{tot}}(q)$  is the total energy of the defect (calculated from first principles as described below) and  $n_X$  and  $\mu_X$  are the number and chemical potential of atoms of species  $X$ , respectively.  $E_F$  is the Fermi energy which is set to zero at the valence-band maximum. In evaluating the chemical potentials, which depend on the experimental growth conditions, we assume thermal equilibrium, e.g.,  $\mu_{\text{Ga}} + \mu_{\text{N}} = \mu_{\text{GaN}}$  for GaN, and  $\mu_{\text{Al}} + \mu_{\text{N}} = \mu_{\text{AlN}}$  for AlN. For convenience, we will display results for metal-rich conditions:  $\mu_{\text{Ga}}$  is put equal to the energy of bulk Ga, or  $\mu_{\text{Al}}$  is put equal to the energy of bulk Al. N-rich conditions would correspond to the chemical potential  $\mu_{\text{N}}$  being determined by the energy of an  $\text{N}_2$  molecule. The chemical potentials for the impurity species (O, Si, and Mg) are fixed by invoking equilibrium with  $\text{Ga}_2\text{O}_3$ ,  $\text{Al}_2\text{O}_3$ ,  $\text{Si}_3\text{N}_4$ , and  $\text{Mg}_3\text{N}_2$ . Formation energies for general values of the chemical potential can always be obtained by referring back to Eq. (2).

The first-principles calculations from which we derive the energies needed in Eq. (2) are based on density-functional theory within the local density approximation (LDA) and the pseudopotential-plane-wave method [6, 7]. We employ a supercell approach and use a tight-binding initialization scheme for the electronic wave functions [8]. Supercells containing 32 atoms were used to study the zinc-blende phase, and up to 96 atoms for the wurtzite phase. An energy cutoff of 40 Ry was used for AlN, with two or three special  $k$  points in the irreducible part of the Brillouin zone. For GaN, a cutoff of 60 Ry is necessary when the Ga 3d electrons are explicitly included as valence electrons. Alternatively, the effects of these  $d$  states can be approximately treated using the nonlinear core correction (nlcc), in which case a 40 Ry cutoff suffices. A discussion of differences between the different approaches (nlcc vs. explicit inclusion of 3d) was given in Ref. [9]. The pseudopotentials were created using the scheme of Troullier and Martins [10].

### 3. $n$ -type doping

#### 3.1. Nitrogen vacancies versus unintentional impurities

All nitrides exhibit a tendency to be  $n$ -type conductive if no special precautions are taken. This was long thought to be caused by the spontaneous formation of nitrogen vacancies. Our first-principles calculations [1, 3] showed, however, that nitrogen vacancies are unlikely to form in  $n$ -type material. The observed  $n$ -type conductivity must therefore be attributed to unintentional incorporation of dopant impurities.

Our first-principles studies [1, 3] as well as those of others [11–13] have shown that the formation energy of the nitrogen vacancy in  $n$ -type GaN is too large for this defect to occur in any appreciable concentrations. We have obtained similar results for the nitrogen vacancy in AlN [4] and in InN [5]. Figure 1 summarizes our first-principles results for native defects and impurities relevant for  $n$ -type GaN and AlN. Many useful results for AlGaN alloys can be obtained by “interpolating”

between the binary compounds. For each defect we only show the line segment corresponding to the charge state that gives rise to the lowest energy at a particular value of  $E_F$ . The change in slope of the lines therefore represents a change in the charge state of the defect [see Eq. (2)]:  $\text{Si}_{\text{Ga}}$ ,  $\text{O}_{\text{N}}$ , and  $\text{V}_{\text{N}}$  all appear with slope +1, indicating single donors. It is clear that O and Si have much lower formation energies than  $\text{V}_{\text{N}}$ ; these impurities can therefore be readily incorporated in *n*-type GaN and AlN. Both O and Si form shallow donors in GaN.

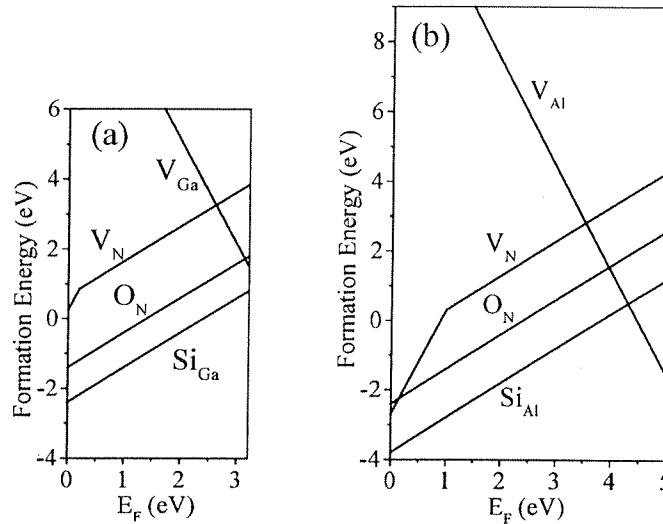


Fig. 1. Formation energies as a function of the Fermi level for defects and impurities relevant for *n*-type material, obtained from first-principles calculations for the zinc-blende phase; (a) is for GaN, (b) for AlN. Metal-rich conditions are assumed. The zero of the Fermi energy is chosen at the top of the valence band. The range of the Fermi levels spans the theoretical band gap.

Figure 1 clearly shows that the formation energy of the nitrogen vacancy is significantly higher than that of oxygen and silicon, which behave as shallow donors. This indicates that the nitrogen vacancy is not the dominant center responsible for the *n*-type conductivity of GaN or  $\text{Al}_x\text{Ga}_{1-x}\text{N}$ .

As early as 1983, oxygen had been proposed as a potential source of *n*-type conductivity in GaN [14]. In 1992, Chung and Gershenson observed the effect of oxygen on the electrical and optical properties of GaN grown by MOCVD [15]. Oxygen was introduced through intentional injection of water. The carrier concentrations in their samples decreased when the growth temperature was increased, a behavior inconsistent with nitrogen vacancies as the cause of the conductivity. Rather, they proposed that less oxygen was being incorporated at the higher growth temperatures.

Nevertheless, the prevailing conventional wisdom, attributing the *n*-type behavior to nitrogen vacancies, proved hard to overcome. Recent experiments have confirmed that unintentionally doped *n*-type GaN samples contain silicon or oxygen concentrations high enough to explain the electron concentrations. Götz

et al. [16, 17] reported electrical characterization of intentionally Si-doped as well as unintentionally doped samples, and concluded that the *n*-type conductivity in the latter was due to silicon. They also found evidence of another shallow donor with a slightly higher activation energy, which was attributed to oxygen. Secondary-ion mass spectroscopy (SIMS) on HVPE material also shows levels of oxygen or silicon in agreement with the electron concentration determined by electrical measurements [17].

High levels of *n*-type conductivity have traditionally been found in GaN bulk crystals grown at high temperature and high pressure [18]. High-pressure studies have recently established that the characteristics of these samples are very similar to epitaxial films that are intentionally doped with oxygen [19, 20]. The *n*-type conductivity of bulk GaN can therefore be attributed to unintentional oxygen incorporation.

Oxygen contamination is often hard to avoid, even in growth environments that are traditionally regarded as very pure. The contaminating impurities may have many sources: water is the main contaminant of  $\text{NH}_3$ , the most frequently used source in MOCVD. Piner et al. [21] pointed out that even high-purity (99.999%)  $\text{NH}_3$  can be a significant source of oxygen contamination, in the case of InGaN growth. Fortunately, purification can remove most of the water. In molecular beam epitaxy (MBE), oxygen may enter as a contaminant in the nitrogen source gas; or it may be due to the quartz lining of certain components, for instance plasma sources.

Kim et al. [22] used the SIMS and Hall effect measurements to investigate the incorporation of various impurities in GaN grown by reactive MBE. They interpreted their results as favoring the nitrogen vacancy as the cause of the unintentional *n*-type conductivity, but acknowledged that the particular set of samples used in their study was not well suited to rule out oxygen contamination. In fact, all of their samples contained sufficient oxygen to explain the electron concentration; therefore their results are entirely *consistent* with oxygen being the donor. Kim et al. observed, however, that the electron concentration does not increase as the oxygen concentration increases. This has been noted by others, as well [23]; it is indicative of the fact that oxygen incorporates not only on nitrogen sites (where it is an electrically active donor), but also in other forms. This additional oxygen may appear, for instance, in the form of  $\text{Ga}_2\text{O}_3$  precipitates.

### 3.2 Oxygen donors and DX behavior

Oxygen acts as a shallow donor in GaN (at atmospheric pressure) and in AlGaN alloys with Al content up to about 30%. The activation energy of oxygen in GaN has been determined from variable-temperature Hall effect measurements [24] to be 29 meV for a donor concentration  $N_D = 1 \times 10^{18} \text{ cm}^{-3}$ . This activation energy decreases with increasing donor concentration. Götz et al. also reported that the total oxygen concentration (measured by SIMS) was significantly higher than the donor concentration. We suggest that such additional oxygen may occur in the form of  $\text{Ga}_2\text{O}_3$  precipitates.

Hydrostatic pressure has been used as a very useful tool to explore the cause and behavior of *n*-type conductivity in GaN [25]. Freeze-out of carriers was re-

ported under application of hydrostatic pressure greater than 20 GPa. These findings can be explained by the behavior of oxygen, which undergoes a transition from a shallow to a deep DX center in wurtzite GaN under pressure [19, 26, 27]. The behavior is similar to that of Si in GaAs. The stable shallow center at the *equilibrium* volume of GaN corresponds to oxygen at the substitutional nitrogen site. The DX geometry corresponds to an oxygen atom moving off the substitutional position along the [0001] direction. This geometry becomes stable under hydrostatic pressure. The associated induced electronic state is a highly localized deep level. In the DX configuration the defect is negatively charged, i.e., it is a deep acceptor, and will therefore trap free carriers. The stability of the localized deep DX state is attributed to interactions between the negatively charged oxygen impurity and a third-nearest-neighbor cation along the *c* axis: we have proposed that a Coulombic attraction is the driving force for the large lattice relaxation that stabilizes the DX geometry [26]. In the zinc-blende structure, these third-nearest-neighbor atoms occur in different positions in the lattice; the formation of the DX configuration is correspondingly suppressed in the zinc-blende phase.

### 3.3. Doping of AlGa<sub>x</sub>N alloys

Several experimental studies have indicated a decrease in *n*-type conductivity of Al<sub>*x*</sub>Ga<sub>1-*x*</sub>N with increasing *x*. Koide et al. [28] reported a decline in free electron concentration for *x* > 0.2. For unintentionally *n*-type doped AlGa<sub>*x*</sub>N, Lee et al. [29] reported a rapid decrease in conductivity for *x* > 0.4. In our own studies [30] we have found a significant decrease in conductivity for *x* > 0.3 in unintentionally doped AlGa<sub>*x*</sub>N samples; the unintentional conductivity was attributed to oxygen. We also found that intentional doping with silicon produced highly conductive material for *x* = 0.44. Bremser et al. [31, 32] also achieved intentional *n*-type doping with silicon up to *x* = 0.42, but for *x* > 0.42 addition of Si resulted in highly resistive films.

Most of these experimental results can be understood by invoking the DX behavior of the oxygen donors. Alloying with AlN increases the band gap of GaN in a similar way to hydrostatic pressure. DX center formation is therefore also expected to occur in Al<sub>*x*</sub>Ga<sub>1-*x*</sub>N. Indeed, our computational studies showed that the DX configuration is the stable state for the oxygen impurity in wurtzite (but not zinc-blende) AlN [26]. Figure 2 shows a configuration coordinate diagram for oxygen displacements in AlGa<sub>*x*</sub>N. The data points were obtained from first-principles calculations for oxygen in GaN and in AlN, based on an interpolation for the case where the DX configuration is 0.1 eV lower in energy than the substitutional donor.

The configuration coordinate diagram displayed in Fig. 2 is characteristic of a metastable center: for zero displacement, the impurity is located on the substitutional site and behaves as a shallow donor. However, a second minimum occurs in the diagram, corresponding to a large displacement of the impurity (close to 1 Å) and a different (negative) charge state. For *x* < 0.3, this second minimum is higher in energy than the on-site, shallow-donor configuration. However, for *x* > 0.3, the second minimum becomes lower in energy, as illustrated in Fig. 2. The DX state

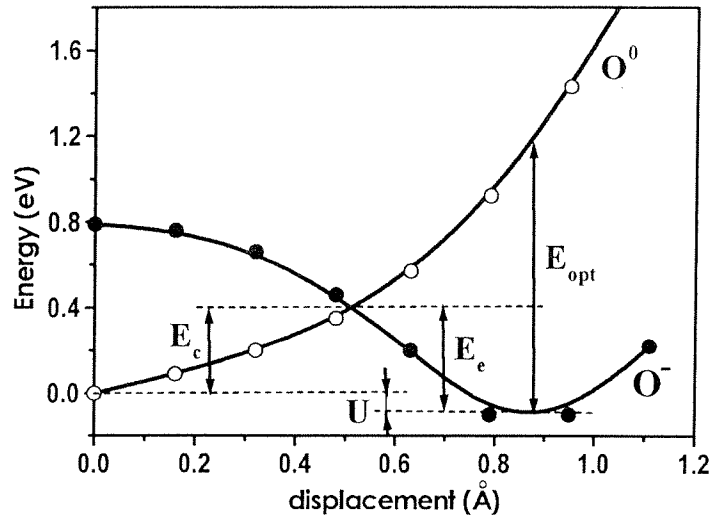


Fig. 2. Configuration coordinate diagram for oxygen displacements along [0001] in AlGaIn, based on first-principles calculations for GaN:O and AlN:O.  $E_{\text{opt}}$  is the optical ionization energy;  $E_c$  and  $E_e$  are the capture and emission barriers.

is then the lowest-energy state of the system; however, electrons can be emitted out of the DX state, and since there is a barrier ( $E_c$ ) to capturing them again, one expects to observe persistent photoconductivity, at least at low temperatures. The mechanism to release electrons out of the DX state can be either thermal (with an activation energy  $E_e$ ) or optical, with a threshold  $E_{\text{opt}}$ .

This model has been experimentally confirmed by the Hall effect and persistent photoconductivity measurements on unintentionally doped AlGaIn samples with Al content up to  $x = 0.39$  [30]. The samples were MOCVD grown, with a thickness of 1  $\mu\text{m}$ , and Al concentrations were determined by X-ray diffraction, assuming relaxed layers and Vegard's law. Concentrations of Si and oxygen impurities were measured by SIMS. Unintentionally doped AlGaIn showed oxygen concentrations of about  $10^{19} \text{ cm}^{-3}$  and silicon concentrations of  $10^{18} \text{ cm}^{-3}$ , indicating that the conductivity of the samples was due to oxygen. Variable-temperature Hall effect measurements showed a freeze-out of the free electrons with decreasing temperature, characterized by an activation energy that increased with Al concentration in the alloy. The activation energy  $E_{\text{DX}}$  was determined by exponential fits to the Hall effect data. The decrease in the free electron concentration can be explained by an increase in  $E_{\text{DX}}$ . This increase in the donor binding energy is consistent with a deep DX level which becomes stable (has a lower energy than the conduction-band minimum) for  $x > 0.27$ , in good agreement with the theoretical prediction. This result is also consistent with the experiments on GaN:O under pressure: the band gap of GaN at 20 GPa is approximately 0.8 eV higher than at ambient pressure, and a similar increase in band gap is found when alloying with AlN with  $x$  between 0.3 and 0.4.

Persistent photoconductivity was observed in  $\text{Al}_x\text{Ga}_{1-x}\text{N}$  epilayers with  $x \geq 0.39$  at temperatures below 150 K. Persistent photoconductivity is a direct

manifestation of metastability, characteristic of centers with a large difference in lattice relaxation between two metastable states. The persistent photoconductivity decreases with time, because oxygen centers return from the shallow to the deep state. In doing so, they need to surmount the barrier (Fig. 2). The temperature range in which this transition was observed was between 120 and 150 K; this is consistent with the barrier  $E_c$  of about 0.4 eV emerging from our calculations. To measure the optical cross-section of absorption for the DX centers, the photocurrent was measured for photon energies from 1.0 to 1.5 eV. An optical threshold of about 1.3 eV was found, again in good agreement with the theoretical prediction shown in Fig. 2.

Observation of persistent photoconductivity is one of the distinguishing features of metastable DX centers; however, it should be noted that persistent photoconductivity is not *necessarily* indicative of the presence of DX-like centers. Various groups have reported persistent photoconductivity in *n*-type GaN [33, 34]. Those observations show photoconductivity at room temperature, while our observations for DX centers only show photoconductivity for temperature below 150 K. In addition, the optical absorption threshold was found to be greater than 2 eV, again inconsistent with the observations for DX centers. The behavior observed in Refs. [33] and [34] may be due to other types of point defects, or to the presence of defective regions near extended defects.

We must conclude that oxygen cannot be used as a shallow donor in  $\text{Al}_x\text{Ga}_{1-x}\text{N}$  with  $x > 0.3$ . Even if another donor impurity is used (such as silicon, see below) that does not exhibit DX behavior, the presence of oxygen in the layer could be detrimental to *n*-type conductivity: indeed, once oxygen undergoes the DX transition it behaves as an acceptor, and therefore counteracts the electrical activity of other donors. Control of oxygen incorporation in  $\text{Al}_x\text{Ga}_{1-x}\text{N}$  with high Al content is therefore essential.

### 3.4. Silicon donors

Silicon is almost universally used for intentional *n*-type doping of GaN, AlGaN, and InGaN. Silicon doping is typically achieved by flowing  $\text{SiH}_4$  during MOCVD growth, or using a solid Si source in MBE. The formation energies shown in Fig. 1 show that the formation energy of silicon is quite low, and therefore it is readily incorporated in AlN as well as in GaN. The activation energy of silicon in GaN derived from the variable-temperature Hall effect measurements [16, 24] is 17 meV for  $N_D = 3 \times 10^{17} \text{ cm}^{-3}$ . As pointed out for oxygen, the ionization energy is sensitive to the concentration of the dopant.

Our calculations for silicon in GaN under pressure, and in AlN, indicate that silicon donors do not exhibit the DX transition [26]. The difference between oxygen and silicon can be understood on the basis of the different location in the lattice. While oxygen substitutes on a *nitrogen* site, silicon sits on a substitutional *cation* site. In that position, the third nearest neighbor is a *nitrogen* atom. In the DX state, the silicon would become negatively charged, and would thus experience a Coulomb repulsion from the third-nearest-neighbor anion; this repulsion suppresses the DX formation. Silicon was indeed experimentally found to remain a shallow donor in



GaN under pressure up to 25 GPa [19]. For  $\text{Al}_x\text{Ga}_{1-x}\text{N}$  alloys with  $x = 0.44$  we found that intentional doping with silicon resulted in a free-electron concentration close to the silicon concentration ( $8 \times 10^{18} \text{cm}^{-3}$ , as measured by SIMS). It was also found, however, that even in the intentionally Si-doped sample a background of oxygen was present (at a level of  $3 \times 10^{18} \text{cm}^{-3}$ ). Those oxygen atoms can still undergo the DX transition, effectively becoming compensating centers. It is important, therefore, to suppress oxygen incorporation when growing Si-doped  $\text{Al}_x\text{Ga}_{1-x}\text{N}$  with high  $x$ . Recently, silicon has been observed to remain a shallow donor in  $\text{Al}_x\text{Ga}_{1-x}\text{N}$  alloys with  $x$  up to 0.60 [2].

The effect of unintentional oxygen incorporation on the conductivity of Si-doped AlGaN is a likely explanation for the experimental observations of Polyakov et al. [35, 36]. They found that the free electron concentration decreases with increasing Al content of the alloy. The increase in Al content also led to an increase in the density of defects with energy levels deeper than silicon, leading to increased difficulty in  $n$ -type doping of the alloy. Polyakov et al. also reported persistent photoconductivity in their samples. These observations can be consistently explained by assuming that oxygen is unintentionally incorporated, a possibility that was recognized by Polyakov et al. The decrease in electron concentration for  $x \geq 0.3$  is then due to the formation of oxygen DX centers; in the negatively charged DX state, oxygen effectively acts as an acceptor, compensating the  $n$ -type conductivity introduced by the Si donors. The characteristics of the persistent photoconductivity (capture and emission barrier, and optical ionization energy) are consistent with those obtained for oxygen DX centers [30] and in our first-principles calculations (see Fig. 2).

Unintentional incorporation of oxygen may also explain the decrease in  $n$ -type conductivity in Si-doped  $\text{Al}_x\text{Ga}_{1-x}\text{N}$  for  $x > 0.42$  observed by Bremser et al. [31, 32]. Even in the absence of oxygen, however, a compensation mechanism may occur, namely due to cation vacancies. In GaN, compensation of Se donors by Ga vacancies was observed by Yi and Wessels [37]. The calculated defect formation energy for the Al vacancy is shown in Fig. 1, for Al-rich conditions in AlN. For  $n$ -type conditions ( $E_F$  high in the gap), silicon donors will suffer from some degree of compensation by triply ionized Al vacancies. The behavior of  $V_{\text{Al}}$  is similar to  $V_{\text{Ga}}$  in GaN [3], but because of the larger band gap of AlN the formation energy of  $V_{\text{Al}}$  in AlN becomes significantly lower than that of  $V_{\text{Ga}}$  in GaN for Fermi-level positions high in the gap (see Fig. 1). Cation vacancies thus become an increasingly important source of donor compensation as the Al content  $x$  is increased in  $\text{Al}_x\text{Ga}_{1-x}\text{N}$ .

## 4. $p$ -type doping

### 4.1. Magnesium in GaN and AlN

The large ionization energy of Mg (around 200 meV) poses severe limitations on the ability to dope GaN, and this problem increases with increasing Al content in AlGaN alloys. We have performed extensive investigations for Mg, as well as various other candidate acceptors, addressing criteria such as solubility,

ionization energy, and potential compensation due to interstitial configurations of the acceptor impurity.

Magnesium is currently the *p*-type dopant of choice for GaN. *p*-type doping of pure GaN was originally a grave problem, but those difficulties have largely been overcome due to the use of the Mg acceptor and the understanding of the role of hydrogen [38, 39]. Still, the hole concentration that can be achieved is lower than desired, particularly for applications such as high *p*-type doping near metal contacts for improved Ohmic contact behavior. In addition, the hole concentration that can be achieved with Mg doping has been observed to decrease rapidly with increasing Al content  $x$  in  $\text{Al}_x\text{Ga}_{1-x}\text{N}$ . Bremser et al. [31, 32] reported a failure to achieve *p*-type conductivity with Mg doping for  $x > 0.13$ . Other studies have also found a decrease in achievable hole concentration when the Al content of the AlGaIn alloy is increased [40–42].

Magnesium exhibits no tendency to form deep levels (so-called AX levels, analogous to DX for donors) [27], thus ruling out a shallow-deep transition as the source of the drop in hole concentration. Figure 3a also shows that incorporation of Mg on interstitial sites, or on nitrogen sites, is energetically unfavorable in GaN [43]. The main issue limiting the hole concentration achievable with Mg in GaN is the solubility.

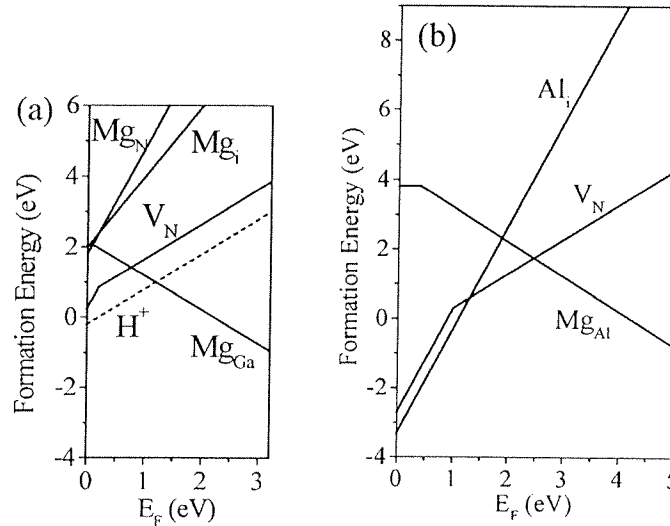


Fig. 3. Formation energies as a function of the Fermi level for defects and impurities relevant for *p*-type material, obtained from first-principles calculations for the zinc-blende phase, and assuming metal-rich conditions; (a) is for GaN, (b) for AlN. The zero of the Fermi energy is chosen at the top of the valence band, and the range of the Fermi levels spans the theoretical band gap. We note that the formation energy of  $\text{Al}_{\text{i}}$  is significantly higher in *wurtzite* AlN. The formation energy of hydrogen donors in GaN is shown in dashed lines.

Our calculations for the Mg acceptor in AlN indicate that its ionization energy (0.4 eV) is higher than in GaN (0.2 eV), as can be seen from Fig. 3 (the ionization energy corresponds to the Fermi level positions where the formation energies of  $\text{Mg}^0$  and  $\text{Mg}^-$  are equal). This increase in the ionization energy leads to a decrease in doping efficiency. Based on an analysis of temperature-dependent Hall data Tanaka et al. found the Mg activation energy to be 35 meV deeper in  $\text{Al}_{0.08}\text{Ga}_{0.92}\text{N}$  than in GaN [40]. Assuming linearity, this would make the Mg acceptor in AlN 0.44 eV deeper than in GaN.

#### 4.2 Nitrogen vacancy defects in *p*-type GaN and AlGaN

Compensation by native defects is another important mechanism that may contribute to the decline in hole concentrations. Figure 3 shows that two defects with low formation energies may inhibit successful *p*-type doping of  $\text{Al}_x\text{Ga}_{1-x}\text{N}$ , namely the nitrogen vacancy and the cation interstitial. The cation interstitial has a low formation energy in zinc-blende AlN, but is much higher in energy in wurtzite. The nitrogen vacancy has a strikingly lower formation energy in AlN than in GaN, and it may play an important role in *p*-type GaN and AlGaN. The formation energy of the nitrogen vacancy is too high for it to be incorporated in *n*-type GaN, but as can be seen from Fig. 3, this formation energy becomes significantly lower in *p*-type material. During MOCVD growth the formation of nitrogen vacancies is suppressed because hydrogen also behaves as a compensating donor, and has a lower formation energy [39]. Still, a certain concentration of nitrogen vacancies will be incorporated, and we propose that these vacancies are at least partially responsible for the decreased doping efficiency of Mg when the Al content is raised in  $\text{Al}_x\text{Ga}_{1-x}\text{N}$  alloys.

The nitrogen vacancy ( $V_{\text{N}}$ ) is a donor which can donate one, two, or three electrons. Only the  $V_{\text{N}}^+$  and  $V_{\text{N}}^{3+}$  charge states are found to be stable; the  $V_{\text{N}}^{2+}$  state is unstable, presenting a so-called negative-*U* effect. This behavior is similar to that calculated for nitrogen vacancies in GaN [44]. However, the  $+/3+$  transition level occurs at a higher position in the band gap in the case of AlN (around 1 eV, see Fig. 3). Because the formation energy decreases much faster with decreasing Fermi level in the  $3+$  charge state, the nitrogen vacancy becomes much more favorable for low Fermi-level positions in AlN.

The  $+/3+$  transition is characterized by a large lattice relaxation [44]. Defects with large lattice relaxations are often responsible for persistent photoconductivity (as we saw in the case of oxygen DX centers). The presence of nitrogen vacancies may therefore be responsible for the observed persistent photoconductivity effects in *p*-type GaN [45, 46]. The nitrogen vacancy may also give rise to the blue lines (around 2.9 eV) commonly observed by photoluminescence in Mg-doped GaN [27, 46–49]. The appearance and disappearance of photoluminescence (PL) lines during post-growth annealing of Mg-doped layers grown by MOCVD [50, 51] may be related to the interactions of hydrogen with nitrogen vacancies. Complexes between hydrogen and nitrogen vacancies can form during growth [52]; the calculated binding energy of the  $V_{\text{N}}-\text{H}^{2+}$  complex, expressed with respect to interstitial H in the positive charge state, is 1.56 eV. Dissociation of this complex, producing

isolated nitrogen vacancies, may explain the behavior of PL lines during annealing for acceptor activation [52].

#### 4.3. Complex formation between magnesium and oxygen

In Sec. 3 we emphasized the tendency of oxygen to incorporate in nitrides, because of its relatively low formation energy. Inspection of Fig. 1 shows that the formation energy of oxygen becomes lower when the Fermi level is lower in the gap; this means that oxygen incorporation will be increasingly favorable when the material becomes *p*-type. This finding clearly highlights the need to control oxygen in the growth system, particularly when growing *p*-type material.

Since oxygen acts as a donor ( $O^+$ ), and Mg as an acceptor ( $Mg^-$ ), these two impurities will be Coulombically attracted to one another. We have performed first-principles calculations of the binding energy of the Mg-O complex, resulting in a value of 0.6 eV (both in GaN and in AlN) [53]. Both magnesium and oxygen lead to an outward relaxation of host atoms; placing Mg and O on adjacent lattice sites is therefore not particularly favored from the point of view of lattice relaxation. This may explain the modest value of the binding energy. Mg moves outward along the Mg-O axis by about 0.10 Å (measured from the ideal lattice site), and oxygen by about 0.15 Å.

The value of the binding energy is actually not large enough to ensure binding of the complex at high temperatures (such as those employed in MOCVD, or in high-pressure bulk growth). Configurational entropy indeed favors formation of isolated centers, as opposed to complexes; only when the binding energy exceeds the formation energy of at least one of the components does complex formation become more likely. Also, since barriers for impurity diffusion are generally expected to be high, we do not expect significant diffusion (from which complex formation could result) during the cool-down process; i.e., the impurities will be “frozen in” in their non-complexed state. Bulk equilibrium considerations therefore indicate that magnesium and oxygen will not form complexes when incorporated at MOCVD growth temperatures or above. These observations, of course, do not exclude the possibility that kinetically-driven processes on the surface could lead to preferential incorporation of Mg-O complexes. To our knowledge, however, no experimental evidence of such complexes exists.

We also note that the tendency of magnesium and oxygen to incorporate in the crystal, when both are present in the growth environment, needs to be balanced against the tendency to form MgO, which acts as a solubility-limiting compound. These driving forces may explain why pressure-growth of GaN single crystals results in samples with significantly lower electron concentrations when Mg is present in the growth solution [54]. Oxygen would normally be incorporated in large quantities, acting as a donor. The presence of Mg results in an additional solubility-limiting phase (MgO), which reduces oxygen incorporation. One expects, though, that a finite concentration of oxygen (as well as Mg) may still be incorporated, with partial compensation of magnesium and oxygen. SIMS studies of Mg and O concentrations in such bulk crystals would be highly informative.

#### 4.4. Complex formation between magnesium and nitrogen vacancies

In Sec. 4.2 we discussed the behavior of nitrogen vacancies as compensating centers in *p*-type nitrides. Since nitrogen vacancies are donors, and Mg is an acceptor, one might again expect a tendency for complex formation. Our calculated binding energy for a neutral  $\text{Mg}_{\text{Ga}}\text{-V}_{\text{N}}$  complex is 0.5 eV, in good agreement with the result of Park and Chadi [27]. Using equilibrium arguments similar to those made for  $\text{Mg}_{\text{Ga}}\text{-O}_{\text{N}}$  complexes in Sec. 4.3, we again do not expect  $\text{Mg}_{\text{Ga}}\text{-V}_{\text{N}}$  complexes to be readily formed — unless conditions on the surface prove favorable for kinetically governed incorporation of such complexes.

### 5. Conclusions

A comprehensive investigation of impurities and defects in AlN and GaN has allowed us to draw conclusions about doping limitations. Our results identify two mechanisms that can reduce the *n*-type doping efficiency: (i) in the case of doping with oxygen (the most common unintentional donor), a DX transition occurs which converts the shallow donor into a negatively charged deep level and (ii) cation vacancies ( $V_{\text{Ga}}$  or  $V_{\text{Al}}$ ) act as triple acceptors and increase in concentration with alloy composition *x*. For *p*-type doping, we find that (i) nitrogen vacancies act as compensating centers and are more easily formed in AlN than in GaN; and (ii) the ionization energy of the Mg acceptor increases with alloy composition *x*. Binding energies for  $\text{Mg}_{\text{Ga}}\text{-V}_{\text{N}}$  and  $\text{Mg}_{\text{Ga}}\text{-O}_{\text{N}}$  complexes were reported; they are low enough to render formation of such complexes under equilibrium conditions unlikely.

### Acknowledgments

We gratefully acknowledge collaborations with D.P. Bour, M. Kneissl, W. Walukiewicz, and W. Götz. Chris Van de Walle is grateful to the Fritz-Haber-Institut and the Paul-Drude-Institut, Berlin, for their hospitality. This work was supported in part by DARPA under agreement no. MDA972-96-3-0014. C. Stampfl and J. Neugebauer gratefully acknowledge support from the DFG (Deutsche Forschungsgemeinschaft), and C. Van de Walle from the Alexander von Humboldt Foundation.

### References

- [1] J. Neugebauer, C.G. Van de Walle, in: *Proc. 22nd Int. Conf. on the Physics of Semiconductors, Vancouver 1994*, Ed. D.J. Lockwood, World Scientific, Singapore 1995, p. 2327.
- [2] C. Wetzel, private communication.
- [3] J. Neugebauer, C.G. Van de Walle, *Phys. Rev. B* **50**, 8067 (1994).
- [4] C. Stampfl, C.G. Van de Walle, *Appl. Phys. Lett.* **72**, 459 (1998).
- [5] C. Stampfl, C.G. Van de Walle, *Mater. Res. Soc. Symp. Proc.* **482**, 905 (1998).
- [6] R. Stumpf, M. Scheffler, *Comput. Phys. Commun.* **79**, 447 (1994).
- [7] M. Bockstedte, A. Kley, J. Neugebauer, M. Scheffler, *Comput. Phys. Commun.* **107**, 187 (1997).

- [8] J. Neugebauer, C.G. Van de Walle, *Mater. Res. Soc. Symp. Proc.* **408**, 43 (1996).
- [9] J. Neugebauer, C.G. Van de Walle, *Mater. Res. Soc. Symp. Proc.* **339**, 687 (1994).
- [10] N. Troullier, J.L. Martins, *Phys. Rev. B* **43**, 1993 (1991).
- [11] T. Mattila, R.M. Nieminen, *Phys. Rev. B* **54**, 16676 (1996).
- [12] T. Mattila, R.M. Nieminen, *Phys. Rev. B* **55**, 9571 (1997).
- [13] P. Bogusławski, E.L. Briggs, J. Bernholc, *Phys. Rev. B* **51**, 17255 (1995).
- [14] W. Seifert, R. Franzheld, E. Butter, H. Sobotta, V. Riede, *Cryst. Res. Technol.* **18**, 383 (1983).
- [15] B.C. Chung, M. Gershenson, *J. Appl. Phys.* **72**, 651 (1992).
- [16] W. Götz, N.M. Johnson, C. Chen, H. Liu, C. Kuo, W. Imler, *Appl. Phys. Lett.* **68**, 3144 (1996).
- [17] W. Götz, J. Walker, L.T. Romano, N.M. Johnson, *Mater. Res. Soc. Symp. Proc.* **449**, 525 (1997).
- [18] P. Perlin, T. Suski, A. Polian, J.C. Chervin, W. Knap, J. Camassel, I. Grzegory, S. Porowski, J.W. Erickson, *Mater. Res. Soc. Symp. Proc.* **449**, 519 (1997).
- [19] C. Wetzel, T. Suski, J.W. Ager III, W. Walukiewicz, S. Fisher, B.K. Meyer, I. Grzegory, S. Porowski, in: *Proc. 23rd Int. Conf. on the Physics of Semiconductors, Berlin 1996*, Eds. M. Scheffler, R. Zimmermann, World Scientific, Singapore 1996, p. 2929.
- [20] C. Wetzel, T. Suski, J.W. Ager III, E.R. Weber, E.E. Haller, S. Fischer, B.K. Meyer, R.J. Molnar, P. Perlin, *Phys. Rev. Lett.* **78**, 3923 (1997).
- [21] E.L. Piner, M.K. Behbehani, N.A. El-Masry, J.C. Roberts, F.G. McIntosh, S.M. Bedair, *Appl. Phys. Lett.* **71**, 2023 (1997).
- [22] W. Kim, A.E. Botchkarev, A. Salvador, G. Popovici, H. Tang, H. Morkoç, *J. Appl. Phys.* **82**, 219 (1997).
- [23] W. Götz, L.T. Romano, J. Walker, N.M. Johnson, R.J. Molnar, *Appl. Phys. Lett.* **72**, 1214 (1998).
- [24] W. Götz, R.S. Kern, C.H. Chen, H. Liu, D.A. Steigerwald, R.M. Fletcher, *Mater. Sci. Eng. B*, in press.
- [25] P. Perlin, T. Suski, H. Teisseyre, M. Leszczyński, I. Grzegory, J. Jun, S. Porowski, P. Bogusławski, J. Bernholc, J.C. Chervin, A. Polian, T.D. Moustakas, *Phys. Rev. Lett.* **75**, 296 (1995).
- [26] C.G. Van de Walle, *Phys. Rev. B* **56**, R10 020 (1997).
- [27] C.H. Park, D.J. Chadi, *Phys. Rev. B* **55**, 12 995 (1997).
- [28] Y. Koide, H. Itoh, N. Sawaki, I. Akasaki, M. Hashimoto, *J. Electrochem. Soc.* **133**, 1956 (1986).
- [29] H.G. Lee, M. Gershenson, B.L. Goldenberg, *J. Electron. Mater.* **20**, 621 (1991).
- [30] M.D. McCluskey, N.M. Johnson, C.G. Van de Walle, D.P. Bour, M. Kneissl, W. Walukiewicz, *Phys. Rev. Lett.* **80**, 4008 (1998).
- [31] M.D. Bremser, W.G. Perry, T. Zheleva, N.V. Edwards, O.H. Nam, N. Parikh, D.E. Aspnes, R.F. Davis, *MRS Internet J. Nitride Semicond. Res.* **1**, 8 (1996).
- [32] M.D. Bremser, W.G. Perry, N.V. Edwards, T. Zheleva, N. Parikh, D.E. Aspnes, R.F. Davis, *Mater. Res. Soc. Symp. Proc.* **395**, 195 (1996).

- [33] M.T. Hirsch, J.A. Wolk, W. Walukiewicz, E.E. Haller, *Appl. Phys. Lett.* **71**, 1098 (1997).
- [34] A.E. Wickenden, G. Beadie, D.D. Koleske, W.S. Rabinovich, J.A. Freitas, Jr., *Mater. Res. Soc. Symp. Proc.* **449**, 531 (1997).
- [35] A.Y. Polyakov, M. Shin, J.A. Freitas, M. Skowronski, D.W. Greve, R.G. Wilson, *J. Appl. Phys.* **80**, 6349 (1996).
- [36] A.Y. Polyakov, N.B. Smirnov, A.V. Govorkov, M.G. Mil'vidskii, J.M. Redwing, M. Shin, M. Skowronski, D.W. Greve, R.G. Wilson, *Solid-State Electron.* **42**, 627 (1998).
- [37] G.-C. Yi, B.W. Wessels, *Appl. Phys. Lett.* **69**, 3028 (1996).
- [38] J. Neugebauer, C.G. Van de Walle, *Phys. Rev. Lett.* **75**, 4452 (1995).
- [39] J. Neugebauer, C.G. Van de Walle, *Appl. Phys. Lett.* **68**, 1829 (1996).
- [40] T. Tanaka, A. Watanabe, H. Amano, Y. Kobayashi, I. Akasaki, S. Yamazaki, M. Koike, *Appl. Phys. Lett.* **65**, 593 (1994).
- [41] M. Katsuragawa, S. Sota, M. Komori, C. Anbe, T. Takeuchi, H. Sakai, H. Amano, I. Akasaki, *J. Cryst. Growth* **189/190**, 528 (1998).
- [42] M. Suzuki, J. Nishio, M. Onomura, C. Hongo, *J. Cryst. Growth* **189/190**, 511 (1998).
- [43] J. Neugebauer, C.G. Van de Walle, *Mater. Res. Soc. Symp. Proc.* **395**, 645 (1996).
- [44] J. Neugebauer, C.G. Van de Walle, in: *Festkörperprobleme/Advances in Solid State Physics*, Ed. R. Helbig, Vol. 35, Vieweg, Braunschweig 1996, p. 25.
- [45] J.Z. Li, J.Y. Lin, H.X. Jiang, A. Salvador, A. Botchkarev, H. Morkoç, *Appl. Phys. Lett.* **69**, 1474 (1996).
- [46] C. Johnson, J.Y. Lin, H.X. Jiang, M.A. Khan, C.J. Sun, *Appl. Phys. Lett.* **68**, 1808 (1996).
- [47] M. Leroux, B. Beaumont, N. Grandjean, P. Lorenzini, S. Haffouz, P. Vennéguès, J. Massies, P. Gibart, *Mater. Sci. Eng. B* **50**, 97 (1997).
- [48] U. Kaufmann, M. Kunzer, M. Maier, H. Obloh, A. Ramakrishnan, B. Santic, P. Schlotter, *Appl. Phys. Lett.* **72**, 1326 (1998).
- [49] F. Calle, E. Monroy, F.J. Sánchez, E. Muñoz, B. Beaumont, S. Haffouz, M. Leroux, P. Gibart, *MRS Internet J. Nitride Semicond. Res.* **3**, 24 (1998).
- [50] S. Nakamura, N. Iwasa, M. Senoh, T. Mukai, *Jpn. J. Appl. Phys.* **31**, 1258 (1992).
- [51] W. Götz, N.M. Johnson, J. Walker, D.P. Bour, R.A. Street, *Appl. Phys. Lett.* **68**, 667 (1996).
- [52] C.G. Van de Walle, *Phys. Rev. B* **57**, R2033 (1998).
- [53] C.G. Van de Walle, C. Stampfl, J. Neugebauer, *J. Cryst. Growth* **189/190**, 505 (1998).
- [54] S. Porowski, *J. Cryst. Growth* **189/190**, 153 (1998).